PHYSICAL REVIEW D VOLUME 49, NUMBER 2 15 JANUARY 1994

Microwave anisotropies from texture-seeded structure formation

Ruth Durrer
Universität Zürich, Institut für Theoretische Physik, CH-8001 Zürich, Switzerland

Armando Howard
Princeton University Observatory, Peyton Hall, Princeton, New Jersey 08544

Zhi-Hong Zhou
Universität Zürich, Institut für Theoretische Physik, CH-8001 Zürich, Switzerland
(Received 27 January 1993)

The cosmic microwave anisotropies in a scenario of large-scale structure formation with cold dark matter (CDM) and texture are discussed and compared with recent observational results of the COBE satellite. A couple of important statistical parameters are determined. The fluctuations are slightly non-Gaussian. The quadrupole anisotropy is $1.5\pm1.2\times10^{-5}$ and the fluctuations on an angular scale of 10° are $(3.8\pm2.6)\times10^{-5}$. The COBE results are within about one standard deviation of the typical texture+CDM model discussed in this paper. On $\sim2^\circ$ angular scale, the fluctuations are significantly larger than recent experimental bounds. Collapsing textures are modeled by spherically symmetric field configurations. This leads to uncertainties of about a factor of 2.

PACS number(s): 98.70.Vc, 11.30.Qc, 98.65.Dx, 98.80.Cq

I. INTRODUCTION

Global texture [1] is the latest of a set of models based on a simple physical idea: the Universe begins in a hot, homogeneous state and then, as it cools, undergoes a symmetry-breaking phase transition that leads to the formation of topological defects [2]. These defects induce perturbations that seed the formation of galaxy and large-scale structure. Unlike stable defects (cosmic strings, domain walls, and monopoles), textures are short lived. In a light-crossing time, they collapse producing a singularity for one instant of time and radiate their energy in a spray of Goldstone bosons. They do, however, persist long enough to leave an imprint as compensated perturbations in the matter and radiation density. The simplicity of the texture scenario is appealing: the model has only a single adjustable parameter, the scale of symmetry breaking, which we normalize to obtain the observed galaxy-galaxy correlation function.

In a series of papers, we and our collaborators have examined the texture-seeded $\Omega=1$ cold-dark-matter-(CDM-)dominated cosmogony and found promising results. Analytical studies of galaxy formation in this scenario suggest that the model has several highly attractive features [3]: early star formation, which could reionize the Universe and smear out fluctuations in the microwave background; early formation of galactic spheroids could account for their high mean density without significant dissipation and would provide a fertile environment for the formation of a massive black hole that could power quasars; a galaxy mass function whose slope and amplitude are consistent with observations; and galaxy formation at moderate z. Numerical simulations of the growth of large-scale structure in the texture scenario find striking consistency between theoretical predictions and observations of large-scale structure [4–6]: the galaxy-galaxy correlation function is consistent with observation; the derived galaxy mass function is well fit by observations; the model produces coherent velocity fields on large scales and the angular correlation function of galaxies is consistent with observations.

In this paper, we calculate the signature of microwave background fluctuations induced by texture on the large scales probed by the Cosmic Background Explorer (COBE) and on intermediate angular scales ($\theta\geq2^\circ$). In Sec. II, we present our formalism for calculating the response of dark matter, baryons, and photons to the collapse of a single spherically symmetric texture in an expanding Universe. These calculations extend earlier work [7,8] that calculated the fluctuations induced by a texture in flat space. In Sec. III we describe how we sum over the contributions from many textures and make a synthetic map of the microwave background. Section IV presents our numerical results and conclusions.

II. THE EFFECTS OF THE COLLAPSE OF A TEXTURE

Texture arises when the symmetry-breaking "Higgs" field chooses to lie at different places on its degenerate vacuum manifold in different regions of space during the phase transition. This can produce configurations in which the Higgs field has a nontrivial winding number on the vacuum manifold, which we call a "knot." Such a knot is unstable to collapse—it shrinks until the gradient of the Higgs field becomes large enough that the field lifts off the vacuum manifold for an instant, undoing the knot. This happens when the knot shrinks to a microscopic size, of order the inverse symmetry-breaking scale. After the knot unwinds, the field is free to radiate away completely.

The cosmological evolution of texture is remarkably

simple: in any given horizon volume, there is a fixed probability of the field configuration being wound into a knot [1,9]. Once there is a sufficient winding number density within the horizon, the knots collapse at the speed of light. As the horizon size grows and "connects" new regions, the process repeats in a self-similar manner, with new knots continually collapsing on progressively larger scales. As they collapse, unwind, and radiate away, the knots generate a gravitational field that perturbs the surrounding matter.

In this paper we study the simplest case of texture: that formed by a completely broken global SU(2) symmetry. It is important to notice, however, that the general picture of cosmological texture evolution just discussed is expected to be the same regardless of the "species" of texture. Thus, we expect many of the main features of the resulting structure formation to be species independent. Furthermore, it turns out that for any texture the dynamics of the field is dependent only on the geometry of the vacuum manifold, and cannot be affected by the shape of the Higgs potential or even the symmetry-breaking scale. The latter does enter our scenario as the one "tunable" parameter, but affects only the *amplitude* of the induced fluctuations, not the pattern. We will see that normalizing the fluctuations such that the resulting cosmic structure matches well with observation implies a symmetry-breaking scale quite natural for grand unified theory (GUT) textures.

A. Formalism

In this section, we will present a formalism for calculating the response of matter and radiation to the collapse of a single texture knot. Throughout this paper, we will assume a flat Friedmann universe, $\Omega_{\rm tot}=1$, dominated by CDM and we work with conformal time so that the background metric is given by

$$ds^2=a^2(-dt^2+dx^2) .$$

We will model the effects of texture by considering the response of matter to the collapse of a single spherical texture. This approach has proven fruitful in describing the response of dark matter to texture [6]. The spherically symmetric ansatz for an S^3 texture (i.e., a configuration of a scalar field living on S^3 which winds once around S^3 as r goes from 0 to ∞) unwinding at a given time $t=t_c$ is [7]

$$\phi=\eta^2(\sin\chi\sin\theta\cos\varphi,\sin\chi\sin\theta\sin\varphi,\sin\chi\cos\theta,\cos\chi) , \tag{1}$$

where θ and φ are the usual polar angles and $\chi(r,t)$ has the properties

$$\chi(r=0,t<t_c)=0 ,$$

$$\chi(r=0,t>t_c)=\pi ,$$

$$\chi(r=\infty,t)=\pi .$$

Since the texture seed is already a perturbation, it can be evolved according to the background equation of motion, $\Box\phi-(\phi\Box\phi)\phi=0$, which yields

$$\partial_t^2\chi+2\left[\frac{\dot a}{a}\right]\partial_t\chi-\partial_r^2\chi-\frac{2}{r}\partial r\chi=-\frac{\sin2\chi}{r^2} . \tag{2}$$

The energy-momentum tensor of the texture field,

$$T_{\mu\nu}=\partial_\mu\phi\,\partial_\nu\phi-\tfrac{1}{2}g_{\mu\nu}\partial_\lambda\phi\,\partial^\lambda\phi ,$$

can be parametrized in terms of dimensionless functions:

$$T_{00}=4\eta^2 f_\rho/l^2 , \quad T_{0i}=-4\eta^2 f_{v,i}/l ,$$

$$T_{ij}=4\eta^2[(f_p/l^2-\tfrac{1}{3}\Delta f_\pi)\delta_{ij}+f_{\pi,ij}] ,$$

where

$$\frac{f_\rho}{l^2}=\frac{1}{8}\left[(\partial_t\chi)^2+(\partial_r\chi)^2+\frac{2\sin^2\chi}{r^2}\right] , \tag{3}$$

$$\frac{f_p}{l^2}=\frac{1}{8}\left[(\partial_t\chi)^2-\frac{1}{3}(\partial_r\chi)^2-\frac{2\sin^2\chi}{3r^2}\right] , \tag{4}$$

$$\frac{f_v}{l}=\frac{1}{4}\int_4^\infty(\partial_t\chi)(\partial_r\chi)dr , \tag{5}$$

$$\Delta f_\pi=\frac{1}{4}\left[(\partial_r\chi)^2-\frac{\sin^2\chi}{r^2}\right]+\frac{3}{4}\int_\infty^r\left[(\partial_r\chi)^2-\frac{\sin^2\chi}{r^2}\right]\frac{dr}{r} . \tag{6}$$

The length parameter l is introduced to keep the functions f_ρ to f_π dimensionless. A convenient choice is to set l equal to the typical size of the perturbations, e.g., the horizon size at texture collapse. f_ρ/l^2 and f_p/l^2 are the energy density and isotropic pressure of the texture field. f_v is the potential of the velocity field and f_π is a potential for anisotropic stresses.

Cosmological perturbations are usually split into scalar, vector, and tensor contributions which do not couple to first order (here the terms scalar, vector, and tensor refer to the transformation properties on hypersurfaces of constant time). The split into scalar, vector, and tensor perturbations is nonlocal and thus acausal. But spherically symmetric perturbations are of course always of scalar type (due to the adoption of spherical symmetry, we lose, e.g., all information about gravity waves produced during the collapse). In this case it is very convenient to apply gauge-invariant cosmological perturbation theory which is adapted to a split into scalar, vector, and tensor modes [8,10–12]. In this paper we use the formalism and notation introduced in Ref. [8].

The gravitational field can be described in terms of the gauge-invariant Bardeen potentials Φ and Ψ. The explicit definition of the Bardeen potentials in terms of the metric perturbations is given in Refs. [10–13]. For perturbations which are much smaller than the size of the horizon, $l\ll l_H$, Ψ corresponds to the Newtonian potential, and Φ is related to the perturbation of the three-curvature on hypersurfaces of constant time:

$$-(4/a^2)\Delta\Phi=\delta R^{(3)}+O(l/l_H) .$$

Hence, for subhorizon perturbations of ordinary matter ($|T^{00}|\gg|T^{ij}|$), the well-known Newtonian limit of

Einstein's equations (see, e.g., Ref. [14]) yields

$$\Delta\Phi=-\Delta\Psi \ .$$

Einstein's equations determine the Bardeen potentials induced by the matter perturbations [8]. In addition to texture we want to describe dark matter and radiation. Since dark matter has zero pressure, we just need a variable describing its density perturbation.

By ρ_d we denote the density of dark matter. D is a gauge-invariant combination of the density perturbation, $\delta=(\rho_d-\rho_{d0})/\rho_{d0}$, the potential for the peculiar velocity, lv, $v_i=-lv_{,i}$, and geometric terms.

In this variable, the evolution of dark matter fluctuations is governed by

$$\ddot{D}+(\dot{a}/a)\dot{D}-4\pi G\rho_d a^2 D=\epsilon(f_\rho+3f_p)/l^2 \ , \tag{7}$$

where $\epsilon=16\pi G\eta^2$. A derivation of this equation is presented in Ref. [8]. After decoupling, the evolution of radiation is given by the one particle Liouville equation. Its first-order perturbation yields a differential equation for $\mathcal{M}$, which is a gauge-invariant version of the perturbation of the energy-integrated photon distribution function:

$$\mathcal{M}=\frac{4\pi}{\rho}\int_0^\infty \mathcal{F}p^3dp \ . \tag{8}$$

$\mathcal{M}$ evolves in response to fluctuations in both the Φ and Ψ potentials [15,13]:

$$\dot{\mathcal{M}}+\gamma^i\partial_i\mathcal{M}=4\gamma^i\partial_i(\Phi-\Psi) \ . \tag{9}$$

The unit vector γ denotes the direction cosines of the photon momentum. In spherically symmetric systems, the photon evolution equation (9) reduces to

$$\dot{\mathcal{M}}+\mu\partial_r\mathcal{M}+\frac{1-\mu^2}{r}\partial_\mu\mathcal{M}=4\mu\partial_r(\Phi-\Psi) \ , \tag{10}$$

where μ is the direction cosine of the photon momentum in the direction of $\mathbf{r}$.

The photon evolution equation is more transparent in characteristic coordinates, (t,τ,b) where $b=r\sqrt{1-\mu^2}$ is the impact parameter and $\tau=t-r\mu$ is the time at which the photon is at its minimum distance from the texture, the "impact time." In these variables (10) simplifies to

$$\partial_t\mathcal{M}(t,\tau,b)=4\mu\partial_r(\Phi-\Psi) \ , \tag{11}$$

so that

$$\mathcal{M}(t,\tau,b)=\mathcal{M}(t_0,\tau,b)+4\mu\int_{t_0}^t dt'\partial_r(\Phi-\Psi) \ . \tag{12}$$

To write down the perturbed Einstein equations we have, in principle, to calculate the energy-momentum tensor of radiation from $\mathcal{M}$. But since we are only interested in late times, $\rho_d\gg\rho_\gamma$, we may neglect the contribution of radiation to the density perturbation. The potential Φ is then determined by the texture and dark matter perturbations alone [8]:

$$\Delta\Phi=-\epsilon[f_\rho/l^2+3(\dot{a}/a)f_v/l]-4\pi Ga^2\rho_d D \ . \tag{13}$$

On the other hand, since dark matter does not give rise to anisotropic stresses, we have to take into account the contribution of radiation to the latter. To calculate the anisotropic stresses of radiation we recall the definition of its amplitude Π (see e.g., Refs. [15,13]):

$$\delta T_l^j-\tfrac{1}{3}\delta T_l^l\delta_l^j=p(\Pi_{,l}^{,j}-\tfrac{1}{3}\Delta\Pi\delta_l^j) \ .$$

The anisotropic contributions to the energy momentum perturbations of photons are given by

$$\delta T_l^j-\frac{1}{3}\delta T_l^l\delta_l^j=\frac{\rho_\gamma}{4\pi}\int\left[\gamma_l\gamma^j-\frac{1}{3}\delta_l^j\right]\mathcal{M}\,d\Omega \ .$$

Using these equations and spherical symmetry one finds

$$\Pi''-\frac{\Pi'}{r}=\frac{9}{4}\int_{-1}^1\left[\mu^2-\frac{1}{3}\right]\mathcal{M}\,d\mu=:\frac{9}{2}M_2(r,t) \ . \tag{14}$$

This anisotropy and the anisotropy of the texture field contribute to the sum of the two Bardeen potentials [8]:

$$\Delta(\Psi+\Phi)=-2\Delta(\epsilon f_\pi+\tfrac{4}{3}\pi Ga^2\rho_\gamma\Pi) \ . \tag{15}$$

Inserting the results for

$$\partial_r(\Phi-\Psi)(r(\tau,\mu),t)$$

at a given time step, we can evolve the brightness function $\mathcal{M}$ according to (12). The function $\mathcal{M}$ is very simply related to the temperature perturbation in a given direction in the sky: To see this, let us express the perturbation of the photon distribution function as a perturbation of the temperature:

$$f=f_{(0)}+\delta f=f_{(0)}[p/T(t,r,\gamma)]$$

so that

$$\delta f=\frac{df_{(0)}}{dv}\delta T/T \ .$$

If we now neglect the difference between gauge-invariant and gauge-dependent variables and set $\delta f\equiv\mathcal{F}$, we find from (8) the simple relation $\mathcal{M}=4\delta T/T$. In the gauge-invariant framework, this just means that $\mathcal{M}/4$ is a gauge-invariant variable describing the perturbation of the temperature in a given direction (for a more explicit discussion see Ref. [13]).

We would like to choose initial conditions that are physically plausible. If the phase transition that produced texture occurred in an initially uniform universe, causality requires that there are no geometry fluctuations well outside the horizon [16]. This implies that initially, at $t_i\ll t_{\rm col}$, we must require $\Psi=\Phi=0$. We want to compensate as much as possible of the initial texture fluctuations with an initial dark matter perturbation. Hence, we use, as initial conditions for the density field,

$$D(r,t=t_i)=-\frac{\epsilon}{4\pi Ga^2\rho_d}\left[\frac{f_\rho}{l^2}+\frac{3(\dot{a}/a)f_v}{l}\right] \ . \tag{16}$$

This initial condition implies that metric fluctuations are induced by the differences between the texture equation of state and the equation of state of the background matter. This choice yields $\Phi=0$ at $t=t_i$, but not $\Psi=0$. Because of its equation of state the dark matter cannot

compensate the anisotropic stresses of the texture. We thus must compensate them by an initial photon perturbation. For Ψ to vanish, we have to require, according to (15),

$$\Pi=\frac{3\epsilon}{4\pi G a^2\rho_\gamma}f_\pi \ .$$

Clearly this does not lead to a unique initial condition for $\mathcal{M}$, but if we in addition require the zeroth and first moments of $\mathcal{M}$ to vanish it is reasonable to set

$$\mathcal{M}(r,\mu,t=t_i)=-\frac{15\epsilon}{8\pi G a^2\rho_\gamma}\left[\mu^2-\frac{1}{3}\right]\left[f_\pi''-\frac{1}{r}f_\pi'\right] . \tag{17}$$

Together with initial conditions for the texture field $\chi(r,t=t_i)$, the requirements (16) and (17) and the evolution equations (2)–(15) determine the system which we solved numerically.

B. Texture collapse in flat space

Before we present numerical methods and results, let us briefly discuss the flat space case, where, if we ignore the response of dark matter to the texture, the microwave fluctuations can be calculated analytically. The Bardeen potentials of a self-similar texture collapsing at $t_c=0$ are [8]

$$\Phi=-\frac{\epsilon}{4}\ln\left[\frac{r^2+t^2}{l^2}\right] , \quad \Psi=\frac{\epsilon}{4}\ln\left[\frac{r^2+t^2}{t^2}\right] ,$$

so that (10) turns into

$$\partial_t\mathcal{M}=\frac{-4\epsilon(t-\tau)}{b^2+(t-\tau)^2+t^2}=g(t,\tau,b) . \tag{18}$$

Integrating that over time one finds

$$\mathcal{M}(t,\tau,b)=\mathcal{M}(t_i,\tau,b)+2\epsilon\left[\frac{\tau}{\sqrt{\tau^2+2b^2}}\left[\arctan\frac{2t-\tau}{\sqrt{\tau^2+2b^2}}-\arctan\frac{2t_i-\tau}{\sqrt{\tau^2+2b^2}}\right]-\ln\left[\frac{(2t-\tau)^2+\tau^2+2b^2}{(2t_i-\tau)^2+\tau^2+2b^2}\right]\right] . \tag{19}$$

We are interested in the change of the distribution function due to the collapsing texture and thus want to perform the limit $t\to\infty$, $t_i\to-\infty$, with

$$\lim_{t_i\to-\infty}\mathcal{M}(t_i,\tau,b)=0 .$$

The ln term in (19) then contributes a constant $C=\lim[\ln(t^2/t_i^2)]$ which crucially depends upon how we perform this limit. It can take any value $-\infty\le C\le\infty$. This can happen because the flat space texture is an unphysical infinite energy solution. If we would change the energy momentum tensor in a way that the texture would be "born" some time in the finite past, or if we would compensate it in a consistent way as we do in the expanding Universe, this problem would disappear. For simplicity, and since we are not interested in a τ- and b-independent constant, we just perform the limit $t=-t_i\to\infty$ which yields $C=0$. Then the final change of the distribution function is

$$\Delta\mathcal{M}(\tau,b)=2\epsilon\pi\frac{\tau}{\sqrt{\tau^2+2b^2}} . \tag{20}$$

Since $\mathcal{M}$ describes the fluctuations in the energy density, $\Delta T/T=\Delta\mathcal{M}/4$.

In a flat universe the signal from a texture collapsing at $t=0$ as seen from an observer at time t_0 and distance r_0 would thus be

$$\frac{\Delta T}{T}(\theta)=\frac{\epsilon\pi}{2}\frac{t_0-r_0\cos\theta}{\sqrt{(t_0-r_0\cos\theta)^2+2r_0\sin^2\theta}} , \tag{21}$$

where θ is the angle between the direction of the texture and the line of sight. A similar calculation using a specific gauge but performing a somewhat unphysical limit is presented in Ref. [17]. Unlike in the expanding Universe (see Sec. II C), there is no horizon present in these calculations; thus, photons that pass the texture long before or after collapse, $|t_0|\gg r_0$, are still influenced by it and yield even a maximum temperature shift:

$$\Delta T/T=\pm\epsilon\pi/2 .$$

In the expanding Universe we expect $\Delta T/T$ to achieve a maximum for $r_0\approx t_0-t_c$ and to vanish for $t_0-t_c\gg r_0$.

C. Texture collapse in the expanding Universe

The coupled set of equations that describes the evolution of texture, the fluctuations in the dark matter, the fluctuations in the metric, and the fluctuations in the microwave background in the expanding Universe must be integrated numerically. We use a second-order accurate leapfrog scheme to advance these equations.

We will assume a specific set of initial conditions for the texture field. One of the sources of uncertainty in our calculations of the microwave background is the choice of initial conditions. We have found that different choices of initial conditions can yield microwave fluctuations that differ by $\sim 50\%$ from the values reported here. We choose initial values for χ that confine the fluctuations in χ to a region comparable to the horizon size at collapse:

$$\chi=Ar/r_0+B(r/r_0)^2+C(r/r_0)^3 , \quad r<\alpha r_0 ,$$
$$\chi=\pi , \quad r>\alpha r_0 , \tag{22}$$

where A, B, and C are determined by the requirement

that $\chi-\pi$ and its first and second derivatives vanish at $r=\alpha r_0$. For $\alpha=\frac{4}{3}$ this texture collapses at $t\approx r_0$. In contrast to the self-similar flat space solution given in Refs. [7,8], for this set of initial conditions, f_π does not vanish initially and the $\Psi(t_i)$ contribution must be compensated by a photon anisotropy Π as explained above.

Figure 1 shows the microwave background fluctuations induced by the collapse of the texture as a function of τ for small impact parameter for both the flat space solution (dotted line) and the texture in the expanding Universe. The dotted line in the figure is the flat space result from Sec. II B. Figure 2 shows the microwave background fluctuations induced by texture collapse as a function of impact parameter. Note that significant temperature fluctuations are induced only for photons that pass within the event horizon of the texture.

D. Compensation

In addition to the choice of a sensible initial condition, we must keep in mind that spherical symmetry is an acausal concept. It induces accelerations on superhorizon scales. This is pictured by the dashed line of Fig. 3. There $\Delta T/T$ is shown as a function of the impact time τ at constant time $t\approx t_c$ and impact parameter $b\approx t_c/50$. One sees that photons with an impact time $\tau\approx -40.0 = -t_c$, i.e., photons which had a distance $r > t_c$ from the texture at the time of the big bang, $t=0$ and always moved in the direction opposite to the texture ($\mu\approx 1$), still experience nearly half of the maximum energy shift even though they have never been in causal contact with the region of texture collapse (which at the collapse time, $t=t_c$ encompasses a radius of t_c).

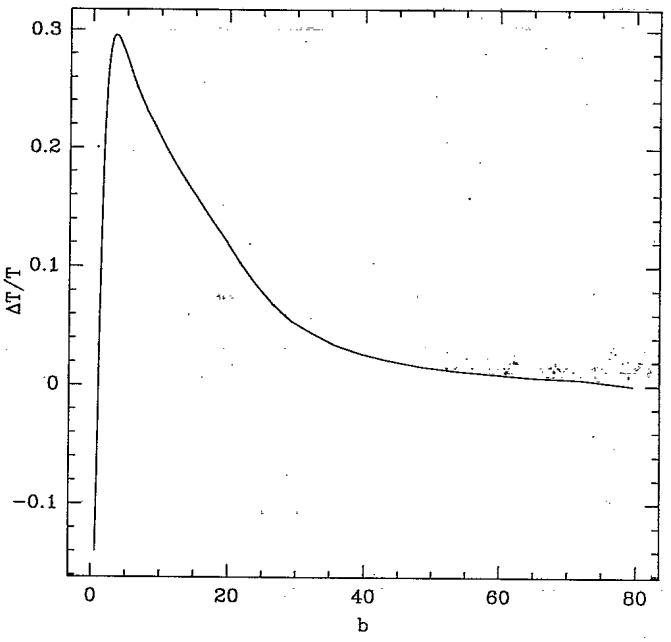

FIG. 2. The CMB perturbation in units of $\epsilon\sim 2.8\times 10^{-4}$ as a function of the impact parameter b for fixed $\tau\sim 0.5t_c=10$. The signal vanishes at an impact parameter $b\sim(1-1.5)t_c$ ($t_c=20$ in the units chosen).

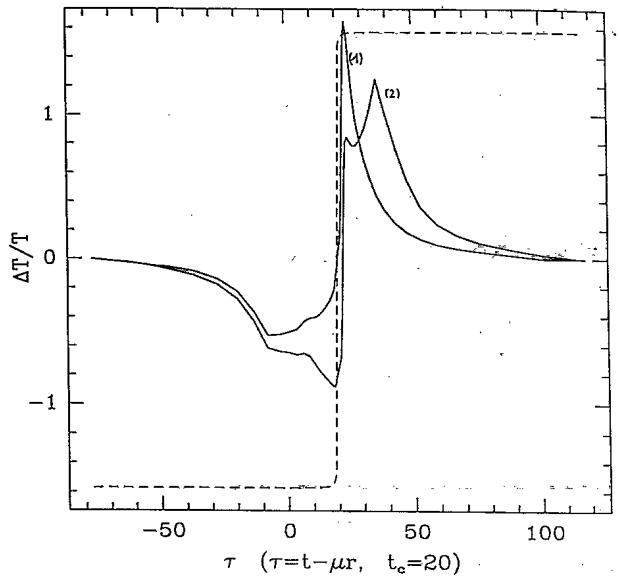

FIG. 1. The hot-spot–cold-spot signal of a spherically symmetric collapsing texture in units of $\epsilon\sim 2.8\times 10^{-4}$. The horizontal variable $\tau=t-r\cos\theta$ denotes the "impact time" (the time of closest encounter with the center of the texture) of a photon arriving at a distance r from the texture at time t traveling with an angle θ with respect to the radial direction. The hot-spot–cold-spot is shown for photons with fixed impact parameter $b=r\sin\theta\approx 0.1t_c$ (t_c is the time of texture collapse). A texture in a recombined expanding universe at $t=t_c$, line (1) and $t=1.5t_c$, line (2) is compared with the flat space result (dashed curve). The second peak appearing at $t=1.5t_c$ is due to the dark matter potential.

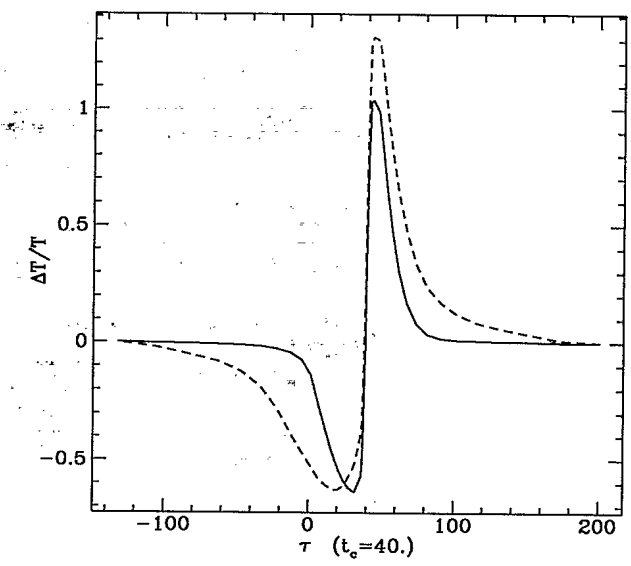

FIG. 3. A comparison of $\Delta T/T$ from a compensated (solid line) and a not compensated (dashed line) texture is shown. The not compensated signal is acausal: a photon which had a distance $\approx -0.5t_c$ from the texture at the time of the big bang ($t=0$) and aways was moving away from it ($\tau\approx -t_c/2$), i.e., never was in causal contact with the texture still experiences about half the maximum energy shift. These acausalities are removed in the compensated case.

These acausalities would lead to an overestimate of $\Delta T/T$. To prevent this we have to compensate in such a way that there are no accelerations on scales larger than the horizon. At each time we thus set the compensation radius equal to the size of the horizon, $r_{cp}=l_H=t$. We then set $f_\rho(r)=f_p(r)=f_v(r)=f_\pi(r)=0$ for $r>r_{cp}$. On small scales we subtract the mean of f_ρ and f_p, so that

$$\int_0^{r_{cp}} f_\rho = \int_0^{r_{cp}} f_p = 0 .$$

A texture compensated in this way does not produce any gravitational fields on scales larger than r_{cp}.

We have added this compensation to the calculation of the texture sources. The signal of a collapsing texture has then reduced to the solid line in Fig. 3. Here photons which have never been and will never be in causal contact with the texture ($\tau<0$) and photons which are not yet in causal contact with the texture ($\tau>2t_c=80$) do not acquire an appreciable energy shift, a result which is much more physical than the dashed line.

Using this compensation scheme, we assume that spherical symmetry is a good approximation inside the horizon and that the stochastic texture field outside the horizon can be neglected. The question if this assumption is justified can only be answered by a full three-dimensional (3D) simulation such as in Ref. [23]. We believe that the issue of compensation and the arbitrariness in the initial conditions yield a factor of about 2 uncertainty in our results (which is much bigger than our numerical errors). It might well be that, by neglecting super-horizon fluctuations completely, we slightly underestimate $\Delta T/T$ but most probably by less than a factor of 2.

III. TEXTURES AND THE MICROWAVE SKY

In the previous section, we described how the collapse of a single texture produces fluctuations in the photon temperature. In this section, we sum the contribution of multiple textures and describe how to construct microwave maps of the night sky.

Since COBE observations cover the entire celestial sphere, we construct a numerical grid consisting of 1 square degree patches. These patches are arranged so that they cover equal areas and each patch has roughly the same shape.

Since the texture fluctuations are in the linear regime, we assume that the contributions of each texture to the fluctuations at each point in the sky can be added independently. We randomly throw down textures everywhere within the event horizon using the texture density distribution function [9],

$$\frac{dn}{dt}=\frac{1}{25}\frac{1}{t^4}, \tag{23}$$

follow the collapse of each texture, and sum their contributions. We include only the contribution of textures that collapse after recombination. Textures that collapse earlier do not contribute significantly to microwave fluctuations on the scales investigated in this paper.

In order to simulate the COBE observations, the map of the night sky is smoothed with a Gaussian beam with a full width at half maximum (FWHM) of 7°, the angular resolution of the Differential Microwave Radiometer (DMR) on COBE [18,19]. After computing and removing the intrinsic dipole contribution (10^{-5}–10^{-4}) and any monopole fluctuations, we then compute the microwave quadrupole, the rms pixel-pixel fluctuations, and other statistics of the microwave sky. The simulated "COBE map" is shown in Fig. 4.

IV. RESULTS

The amplitude of the microwave background fluctuations depends upon the scale of symmetry breaking associated with the texture. If the texture model is normalized so that it can reproduce the galaxy-galaxy correlation function, then $\epsilon=5.6\times10^{-4}b^{-1}$, where b, the bias factor, is the ratio of the mass-mass correlation function to the galaxy-galaxy correlation function [3,24]. Comparison of the predictions of the texture model with observations of clusters [25] suggests that $b\approx2$–4. Hydrodynamical simulations of texture-seeded galaxy formation [5] suggest that $b\approx2$.

Figure 5 shows the distribution of quadrupole values calculated from 100 realizations of the model. Averaging over the realizations, we find an rms value for Q of

$$Q=(1.5\pm1.2)\times10^{-5}\epsilon_0 ,$$

where we have set $\epsilon_0=\epsilon/2.8\times10^{-4}$ so that a bias factor of 2 and the above normalization would yield $\epsilon_0=1$. In 13% of the realizations the calculated value of the quadrupole is below the COBE result ($Q=5\times10^{-6}$). Since only a handful of texture knots are the source of most of the large-scale fluctuations, the quadrupole varies significantly from realization to realization. The 95% confidence range is $3.5\times10^{-6}\epsilon_0$ to $4\times10^{-5}\epsilon_0$. The COBE value is well within one standard deviation.

The texture-induced microwave sky shows non-Gaussian features that distinguish it from the standard inflationary models. Figure 6 shows the distribution of pixel-to-pixel fluctuations calculated in one of the simulations. The dotted line shows a Gaussian whose dispersion matches the temperature dispersion of this simulation. The average temperature fluctuation averaged over 100 simulations is

$$(\Delta T/T)_{rms}(10°)=(3.8\pm2.6)\times10^{-5}\epsilon_0 .$$

This number is consistent with the estimate based on three-dimensional simulations of texture-induced microwave fluctuations [23,24]. Figure 6 shows that the distribution of temperature fluctuations is only mildly non-Gaussian, the skewness of the distributions averaged over 100 realizations is -4 ± 2.3 and the kurtosis of the distributions is 32 ± 29.

Considering these findings, the recently reported results from the COBE differential microwave background radiometers (DMR) [19] are consistent with the texture + CDM scenario. The experiment has measured a value of $Q=(0.5\pm0.1)\times10^{-5}$ for the microwave quadrupole and

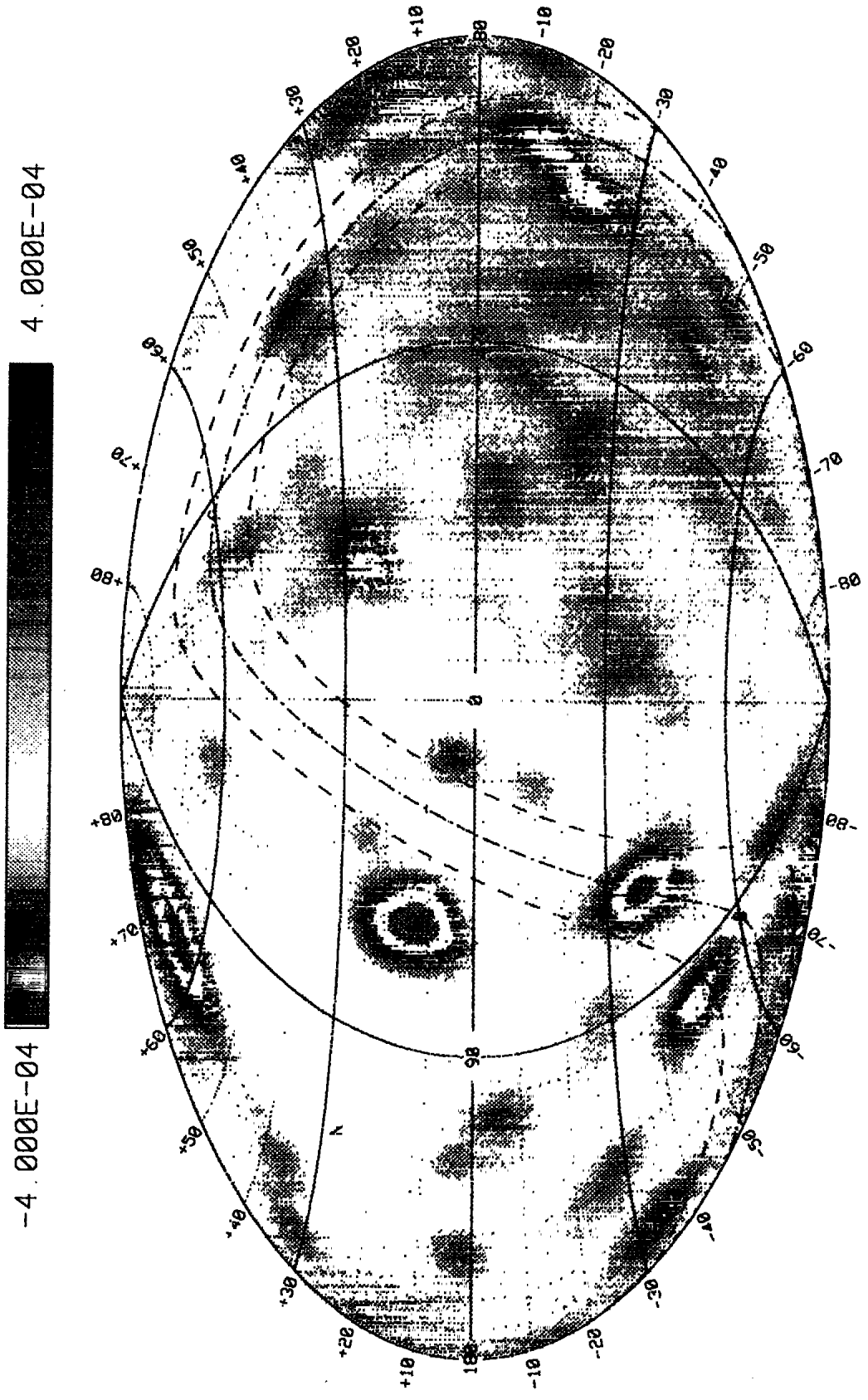

FIG. 4. A simulated COBE map as it might look in a scenario with texture+CDM. The color scheme goes from -4×10^{-4} (dark blue) to 4×10^{-4} (deep red). The zero point is not the middle of the color palette but at the green-yellow transition. Monopole and dipole contributions are subtracted in this map.

$$(\Delta T/T)_{\rm rms}=(1.1\pm0.18)\times10^{-5}$$

for the pixel-to-pixel fluctuations in the microwave maps. Both these values lie within one standard deviation from the results of more than 100 realizations of the texture scenario. (Recent reexaminations of the COBE results suggest that the quadrupole may be somewhat lower [22].) For the texture scenario, this implies that $\epsilon\approx3\times10^{-4}$ and a bias factor of $b\approx2$ are compatible with both the large-scale structure formation and the microwave background anisotropies produced in this scenario.

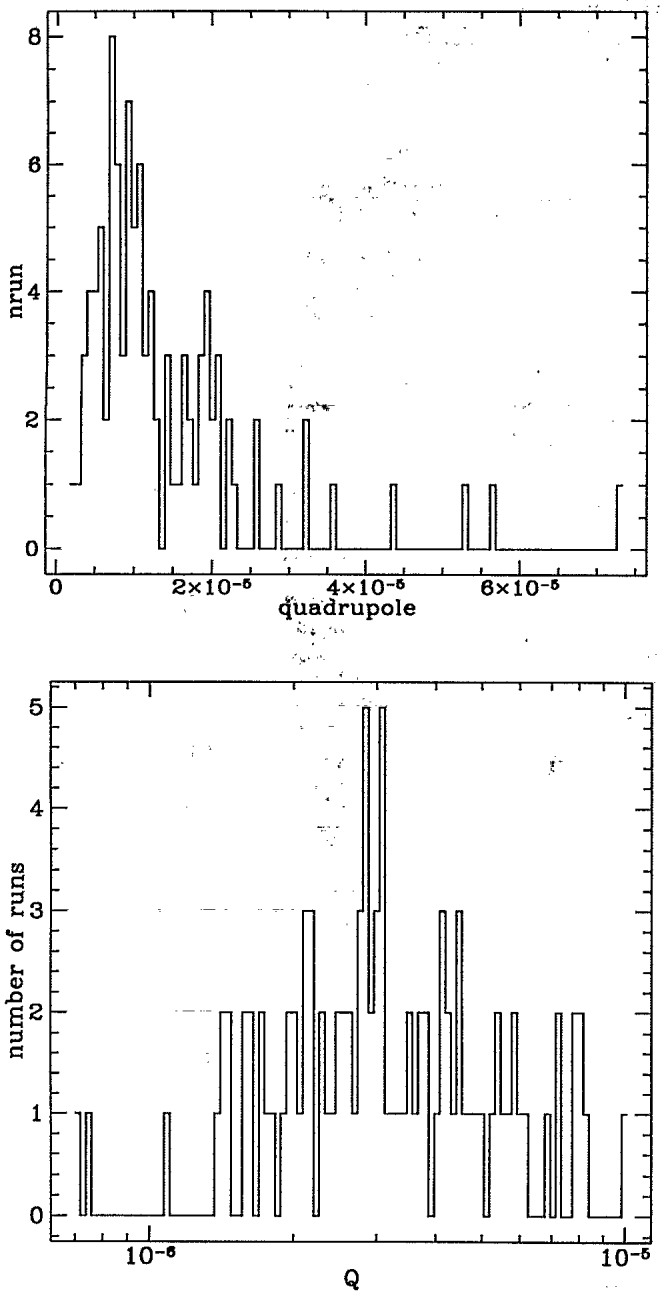

FIG. 5. The distribution of quadrupole values of 100 realizations of the microwave sky is shown in (a) linear and (b) logarithmic scales. The distribution is very broad with an average of 1.5×10^{-5} and a standard deviation of 1.2×10^{-5}.

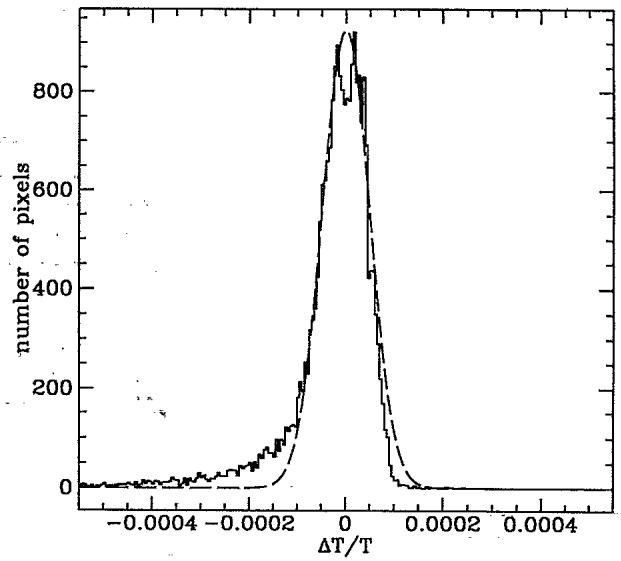

FIG. 6. The statistical distribution of the microwave anisotropies for one realization of the microwave sky. The number of pixels with a given $\Delta T/T$ are counted. The distribution is slightly non-Gaussian, negatively skewed (skewness $=-3$, kurtosis $=-1.2$).

Our simulation does not take into account the baryon-photon coupling before recombination and does not properly model the process of recombination itself. It is thus not well suited to account for textures which collapse before recombination, i.e., for angular scales beyond about $\theta_{\rm min}=2°$. At this minimal resolution, the fluctuations in our simulations are

$$(\Delta T/T)_{\rm rms}(2°)=(3.9\pm0.8)\times10^{-5}\epsilon_0 .$$

It is interesting that the cosmic variance (i.e., difference in values over our 100 realizations for this angle) has now really dropped. This is clear, since more than 1000 textures have contributed to this signal in each map. Our number does contradict the south pole result [20] but is in marginal agreement with the recent Millimeter-Wave-Anisotropy Experiment (MAX) (third flight) [21]. In Fig. 7 the autocorrelation function is shown with 1σ upper and lower limits. On small scales, it is typically a factor of 2–3 higher than the COBE result [19]. This shows that the texture scenario (without reionization) conflicts observations on small scales ($\theta\leq5°$). In Fig. 8 the amplitudes of the spherical harmonics are presented. To specify our conventions, we redefine them here:

$$(\Delta T/T)(\vartheta,\phi)=\sum_{l=0}^{\infty}\sum_{m=-l}^{l}a_{lm}Y_{lm}(\vartheta,\phi)\ , \tag{24}$$

where

$$a_{lm}=\int d\Omega(\Delta T/T)Y_{lm}^{*}\ .$$

The amplitudes C_l are then given by

$$C_l=\frac{1}{2l+1}\sum_{m=-l}^{l}|a_{lm}|^2\ . \tag{25}$$

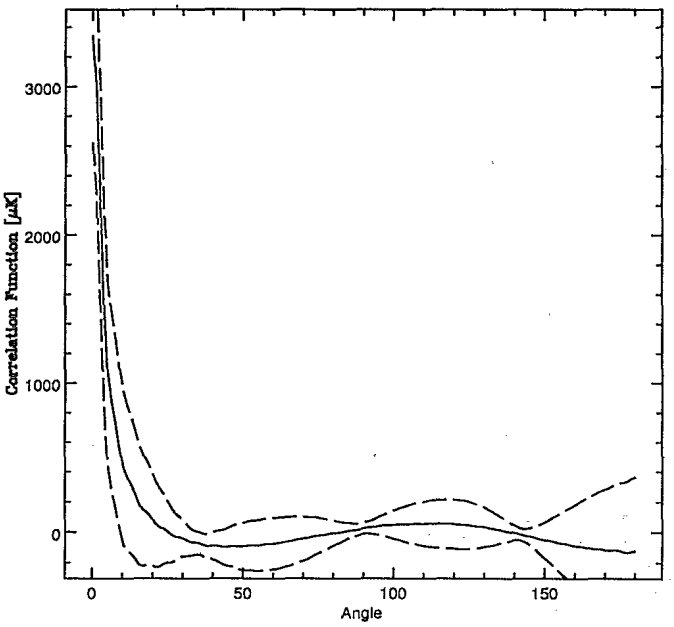

FIG. 7. The autocorrelation function is presented in units $(\mu K)^2$ (for a bias factor of 2, $\epsilon_0=1$, see text). In addition to the values averaged over 100 realizations (solid line), we indicate the 1σ upper and lower limits (dashed lines).

In Fig. 8 we also present, in addition to the values $\langle C_l \rangle$ averaged over 100 realizations, their 1σ upper and lower limits. Furthermore, the analytical fits for power law spectra with $n=1.5$ (short dashed) and $n=1$ (long dashed) are plotted. A simple investigation leads to a 1σ

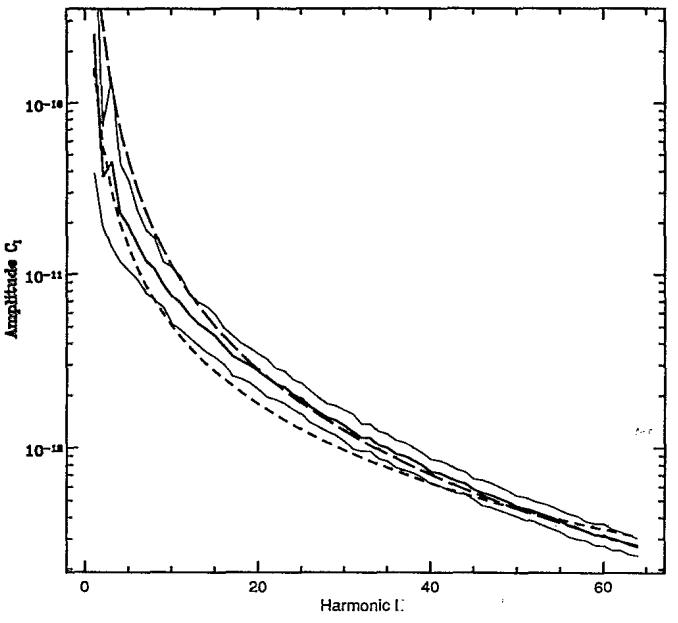

FIG. 8. The amplitudes of the spherical harmonics for $l=2$–64, averaged over 100 simulations are shown (thick solid line) and the 1σ upper and lower limits are indicated (thin solid lines). For comparison we have also plotted the analytical fits for power law spectra with $n=1.5$ (short dashed line) and $n=1$ (long dashed line).

limit of the spectral index of about $n=1.2\pm0.3$, although our numerical result definitely does not represent a pure power law.

Up to now we have only considered the statistical variations of our results which vary accidentally from realization to realization, i.e., cosmic variance. It is, however, important to note that due to the uncertainties in modeling the typical textures and approximations inherent in modeling the texture as spherically symmetric, these estimates of the microwave background fluctuations are uncertain by a factor ~ 2, representing a systematic error. Since in this approximation we completely neglect all nontopological fluctuations of the scalar field, we probably underestimate the induced fluctuations. On the other hand, a different choice for the scalar field leading to a different vacuum manifold M may as well alter the results by a factor of 2 (by altering the probability of texture formation). In addition, we throw down the textures randomly, uncorrelated whereas 3D numerical simulations hint that they are probably anticorrelated.

Because of the non-Gaussian nature of the initial conditions, galaxy formation begins much earlier in the texture model than in Gaussian theories of structure formation. By $z=50$, a fraction 6×10^{-5} of the mass of the Universe has formed nonlinear objects of mass greater than $10^6 M_\odot$—these objects may have reionized the Universe. If 10% of the baryons in these objects are "burnt" in high mass stars, then the resultant energy, 60 eV per baryon, is sufficient to reionize the Universe. The optical depth of an ionized universe is

$$\tau(z)=0.9\times10^{-3}\left[\frac{h_{50}\Omega_b}{0.05}\right][(1+z)^{3/2}-1] \tag{26}$$

so that we get an optical depth of 0.33 back to $z=50$ in an $\Omega_b=0.05$, $h_{50}=1$, and $\Omega=1$ universe. A very rough estimate of the effects of reionization by smoothing each texture with a smoothing scale of about the horizon size at $z_{\rm dec}$, where $z_{\rm dec}$ is determined by $\tau(z_{\rm dec})=1$; thus,

$$z_{\rm dec}=107\left[\frac{0.05}{h_{50}\Omega_b}\right]^{2/3}.$$

This corresponds to an angular scale of

$$\theta_{\rm smooth}=t(z_{\rm dec})/t_0=(1+z)^{-1/2}$$

$$\approx 5.7^\circ\left[\frac{\Omega_b h_{50}}{0.05}\right]^{1/3}. \tag{27}$$

This smoothing length is somewhat larger than the resolution scale of COBE. If the formation of objects leads to reionization prior to $z_{\rm dec}$ this would suppress microwave background fluctuations on the smallest scales investigated in this paper ($\sim 2^\circ$), but would not affect the fluctuations on the larger scales ($\geq 10^\circ$) probed by COBE.

We conclude again that our simulations indicate that the texture scenario can reproduce the CBR anisotropies measured by COBE and no pronounced inconsistencies with the COBE data are found.

Because of the fact that a collapsing texture is a rare event, the rms pixel fluctuations increase slightly at

smaller scales. This leads to an increase by nearly a factor of 2 of the 1σ lower limit of the fluctuation amplitude at 10° to the amplitude at 6°. This can be compensated by the damping of fluctuations due to reionization which can also affect scales which are somewhat larger than θ_{smooth}. To further test this scenario it is important, in addition to a full three-dimensional investigation of the CBR anisotropies, to discuss the damping by reionization in detail for anisotropies on intermediate scales, 1°–5°.

Our work confirms that the texture scenario is a viable candidate for large-scale structure formation which cannot be excluded by present observation. Its CBR anisotropies can be distinguished from those of a scenario with initial fluctuations induced due to an inflationary phase by two statistical criteria: The fluctuations are slightly non-Gaussian and they increase somewhat towards smaller angular scales. A speciality of the texture scenario is furthermore the very distinct signal which one singular texture collapse would imprint on the microwave sky. Depending on the time of texture collapse and on our distance to it, we would see a roughly spherical ring of negative, positive, or negative-positive fluctuation, see Fig. 9. Given the statistical distribution of textures (23), we expect to observe about 5–10 such rings with an angular diameter around 10°.

It is clear that although as a function of the impact parameter the photon signal shows a blueshift followed by a redshift, what is observed at a given moment in the sky is either dominated by redshifted or by blueshifted photons, since most photons arriving at the observer today have impact times which differ by much less than the typical size of the texture. Because of spherical symmetry, the signals form rings in the sky. In a more realistic 3D simulation these rings would be deformed. The blueshifted rings are more affected by compensation and thus less pronounced as seen on the map (Fig. 4).

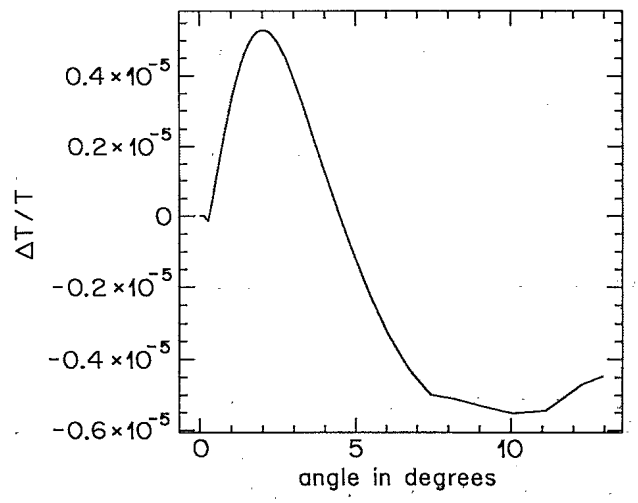

FIG. 9. The spherical ring of positive-negative fluctuation as seen in the microwave sky from a texture collapsing at redshift $z\approx 100$ a distance $r\approx t_0-t_c$ away from the observer.

ACKNOWLEDGMENTS

We would like to thank Lyman Page, Norbert Straumann, and Neil Turok for stimulating discussions. We are very grateful to Ken Ganga who helped us in producing the color map and David Spergel who participated in the first part of this project. R.D. and Z.-H.Z. acknowledge support from the Swiss NSF.

APPENDIX: DAMPING BY PHOTON DIFFUSION

In this appendix we want to estimate the damping of CBR fluctuations in an ionized plasma. For simplicity we work here in physical, not conformal time and we always consider a flat, matter-dominated universe, so that $t=t_0/(1+z)^{3/2}$ and $\rho_\gamma<\rho_b$.

For a perturbation with wave number k which is significantly smaller than the mean free path, the damping rate is then [26]

$$\gamma\approx k^2 t_T/6\ , \tag{A1}$$

where $t_T=1/(\sigma_T n_e)$ is the mean free path of the photons. We now consider a texture which collapses at time $t_c=t_0/(1+z_c)^{3/2}$. The total damping $\exp(-f)$ which this perturbation experiences is given by the integral

$$f\approx\int_{t_c}^{t_{\text{end}}}\gamma(t)dt\ . \tag{A2}$$

The end time t_{end} is the time when the mean free path t_T equals t_c, the size of the perturbation. We define z_{dec} as the redshift when the photons and baryons decouple due to free streaming. This is about the time when the mean free path has grown up to the size of the horizon: $t_T(z_{\text{dec}})\approx t(z_{\text{dec}})$. To obtain exponential damping ($t_c<t_{\text{end}}$), we thus need $z_c>z_{\text{dec}}$. In this case damping is effective until

$$1+z_{\text{end}}=\sqrt{(1+z_{\text{dec}})(1+z_c)}\ ,$$

and we obtain

$$f\approx 2\left[\frac{1+z_{\text{dec}}}{1+z_c}\right]^{3/2}\left[\left[\frac{1+z_c}{1+z_{\text{dec}}}\right]^{9/4}-1\right]\ , \tag{A3}$$

where we have set $k^2/6=(2\pi/t_c)^2$. In terms of angles this yields

$$f(\theta)\approx 2(\theta/\theta_d)^3[(\theta_d/\theta)^{9/2}-1]\ ,$$

where $\theta_d=1/\sqrt{1+z_{\text{dec}}}\approx 5.7°$.

If the plasma ionizes at a redshift z_i, $z_{\text{dec}}<z_i<z_c$, after the texture has already collapsed, damping is only effective after z_i if $z_{\text{end}}<z_i$ and instead of formula (A3) we then obtain

$$f\approx 2\left[\frac{1+z_{\text{dec}}}{1+z_c}\right]^{3/2}\left[\left[\frac{1+z_c}{1+z_{\text{dec}}}\right]^{9/4}-\left[\frac{1+z_c}{1+z_i}\right]^{9/4}\right]\ . \tag{A4}$$

This damping factor can again be converted in an angular damping factor in the above, obvious way. The CBR signal of textures is thus exponentially damped only if

$$z_i > z_{\rm dec} \approx 107(0.05/h_{50}\Omega_b)^{2/3}$$

and in this case only textures with

$$1+z_{\rm dec} < 1+z_c < (1+z_i)^2/(1+z_{\rm dec})$$

are affected. For exponential damping after reionization at $z_i = 50$ extreme values of the Hubble constant and baryon densities far above that predicted from big-bang nucleosynthesis and light element abundances are required.

In this approximation we have neglected the amount of damping which still may occur after $z_{\rm end}$.

[1] N. Turok, Phys. Rev. Lett **63**, 2625 (1989).
[2] T. W. B. Kibble, Phys. Rep. **67**, 183 (1980).
[3] A. Gooding, D. N. Spergel, and N. Turok, Astrophys. J. **372**, L5 (1991).
[4] C. B. Park, D. N. Spergel, and N. Turok, Astrophys. J. **372**, L53 (1991).
[5] R.-Y. Cen, J. P. Ostriker, D. N. Spergel, and N. Turok, Astrophys. J. **383**, 1 (1991).
[6] A. Gooding, C. B. Park, D. N. Spergel, N. Turok, and J. R. Gott III, Astrophys. J. **393**, 42 (1992).
[7] N. Turok and D. N. Spergel, Phys. Rev. Lett. **64**, 2736 (1990).
[8] R. Durrer, Phys. Rev. D **42**, 2533 (1990).
[9] D. N. Spergel, N. Turok, W. H. Press, and B. S. Ryden, Phys. Rev. D **43**, 1038 (1991).
[10] J. Bardeen, Phys. Rev. D **22**, 1882 (1980).
[11] H. Kodama and M. Sasaki, Prog. Theor. Phys. Suppl. **78**, 1 (1984).
[12] R. Durrer and N. Straumann, H.P.A. **61**, 1027 (1988).
[13] R. Durrer, "Fundamentals of Cosmic Physics," report (unpublished).
[14] N. Straumann, *General Relativity and Relativistic Astrophysics*, Texts and Monographs in Physics (Springer, Berlin, 1984).
[15] R. Durrer, Astron. Astrophys. **208**, 1 (1989).
[16] S. Veeraraghavan and A. Stebbins, Astrophys. J. **365**, 37 (1990).
[17] R. Durrer, M. Heusler, P. Jetzer, and N. Straumann, Nucl. Phys. **B368**, 527 (1992).
[18] G. F. Smoot, C. L. Bennett, A. Kogut, J. Aymon, C. Backus, G. De Amici, K. Galuk, P. D. Jackson, P. Keegstra, L. Rokke, L. Tenorio, S. Sottes, S. Gulkis, M. G. Hauseroc, M. A. Jannsen, E. S. Cheng, T. Kelsall, P. Lubin, S. Meyer, S. H. Moseley, T. L. Murdock, R. A. Shafer, and R. F. Silverberg, Astrophys. J. **371**, L1 (1991).
[19] G. F. Smoot *et al.*, Astrophys. J. **396**, L1 (1992); E. L. Wright *et al.*, *ibid.* **396**, L13 (1992).
[20] T. Gaier, J. Schuster, J. Gundersen, T. Koch, M. Seiffert, P. Meinhold, and P. Lubin, Astrophys. J. **398**, L1 (1992).
[21] P. Meinhold *et al.*, Astrophys. J. **409**, L1 (1993); J. O. Gundersen *et al.*, *ibid.* **409**, L5 (1993).
[22] A. Gould, IAS report (unpublished).
[23] D. Bennett and S. Rhee, LBL report (unpublished).
[24] Ue-li Pen, D. N. Spergel, and N. Turok, Phys. Rev. D **49**, 692 (1994).
[25] J. Bartlett, A. K. Gooding, and D. N. Spergel, Astrophys. J. (to be published).
[26] P. J. E. Peebles, *The Large-Scale Structure of the Universe* (Princeton University Press, Princeton, NJ, 1980), Sec. 92C.